



Intelligent PI speed controller for solar cells urbane electric vehicle

Brahim Gasbaoui¹, Abdelfatah Nasri

Faculty of the sciences and technology, Bechar University, B.P 417 BECHAR (08000), ALGERIA

University of E.N.S.E.T, B.P 98 ORAN (31000), ALGERIA

gasbaoui_2009@yahoo.com

Abstract— Currently the researchers of Electric vehicle devotes their time to minimize the time of starting and the acceleration of the electric vehicles to undergo this problem a PI controller optimize by the harmony search (PI-HS) was proposed. The electric vehicle is driving which utilize the two back separately induction motors for motion. The aim object of the ant colony is to give more and more safety for the electric propulsion system safety during motion against road topology. In this work the ant colony optimization has been used to illustrate performance of optimized PI controller parameters of speed controller for EV. It is expected to improve the system performances. The electronic differential system ensures the robust control of the vehicle behavior on the road Computer simulations demonstrate that compared with conventional PI controller, this optimized PI controller has best performances for speed controller and very effective in improving overshoot error and setting time. document gives formatting instructions for authors preparing .

Keywords— Electric vehicle , Electronic differential, PI controller, harmony search ,Solar Panel.

I. INTRODUCTION

Today, automobile transportation is in a crisis with regard to the high price of gasoline. In the future, the crisis will take on unprecedented proportions. Not just apparent; overwhelming. The supply of oil will diminish and hybrid vehicles will play a major role in diffusing the situation in comparison, electric cars were comfortable, quiet, clean, and fashionable. Electric cars did not need to be cranked, a feature especially attractive to women. Ease of control was also a desirable feature. However, as shown in table I, the range was limited by energy storage in the battery. For city use, the range was adequate. After every trip, the battery required recharging. Lead acid batteries were used in 1900. Lead acid batteries are still used in modern cars.

Indirectly driven EVs are powered by electric motors through vehicles are propelled by in-wheel or, simply, wheel motors [1, 2]. The basic vehicle configurations of this research has two directly driven wheel motors installed and operated inside the driving wheels on a pure EV. These wheel motors can be controlled independently and have so quick and accurate response to the command that the vehicle chassis control or motion control becomes more stable and robust, compared to indirectly driven EVs. Like most research on the torque distribution control of wheel motor, wheel motors

[3, 14] proposed a dynamic optimal tractive force distribution control for an EV driven by four wheel motors, thereby improving vehicle handling and stability [4, 5].

The Harmony Search (HS) algorithm is a recently developed meta-heuristic algorithm, and has been very successful in a wide variety of optimization problems. HS was conceptualized using an analogy with music improvisation process where music players improvise the pitches of their instruments to obtain better harmony. The HS algorithm does not require initial values and uses a random search instead of a gradient search, so derivative information is unnecessary. Furthermore, the HS algorithm is simple in concept, few in parameters, easy in implementation, imposes fewer mathematical requirements, and does not require initial value settings of the decision variables [18].

Therefore, harmony search (HS) can be applied in tuning the gains of PI controller to ensure optimal control performance at nominal operating conditions.

The reminder of this paper is organized as follows: Section II reviews the principle components of the electric traction chain with their equations model. Section III shows the mechanical vehicle load modeling. Section IV shows the development of Direct Torque controller detailed for Electric vehicle motorization. The proposed structure of the studied propulsion system is given in the section V. Section VI gives some simulation results of the different studied cases. Finally, the conclusion is drawn in the latest section.

II. ELECTRIC VEHICLE DESCRIPTION

According to Fig. 1 the opposition forces acting to the vehicle motion are: the rolling resistance force F_{tire} due to the friction of the vehicle tires on the road; the aerodynamic drag force F_{aero} caused by the friction on the body moving through the air ; and the climbing force F_{slope} that depends on the road slope [1,2 3].

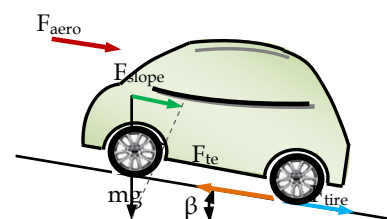


Fig. 1 The Forces Acting on a Vehicle Moving Along a Slope.



The total resistive force is equal to F_r and is the sum of the resistance forces, as in (1).

$$F_r = T_{slope} + T_{tire} + T_{aero} \quad (1)$$

The rolling resistance force is defined by:

$$T_{tire} = mgf_r \quad (2)$$

The aerodynamic resistance torque is defined as follows:

$$F_{aero} = \frac{1}{2} \rho_{air} \cdot A_f \cdot C_d \cdot v^2 \quad (3)$$

The rolling resistance force is usually modeled as:

$$F_{slope} = mg \sin(\alpha) \quad (4)$$

Where m is the total masse of vehicle r is the tire radius, f_r is the rolling resistance force constant, g the gravity acceleration, ρ_{AIR} is Air density, C_d is the aerodynamic drag coefficient, A_f is the frontal surface area of the vehicle, v is the vehicle speed, α is the road slope angle. Values for these parameters are shown in Table1.

TABLE I. PARAMETERS OF THE ELECTRIC VEHICLE MODEL

r	0.32 m	A_f	2.60 m ²
m	1300 Kg	C_d	0.32
f_r	0.01	ρ_{air}	1.2 Kg/m ³

III. HARMONY SEARCH OPTIMIZATION ALGORITHM

GA Recently, Geem et al. [8] developed a new harmony search (HS) meta-heuristic algorithm that was conceptualized using the musical process of searching for a perfect state of harmony. The harmony in music is analogous to the

optimization solution vector, and the musicians' improvisations are analogous to local and global search schemes in optimization techniques. The HS algorithm does not require initial values for the decision variables.

Furthermore, instead of a gradient search, the HS algorithm uses a stochastic random search that is based on the harmony memory considering rate and the pitch adjusting rate (defined in harmony search meta-heuristic algorithm section), so that derivative information is unnecessary.

Compared to earlier meta-heuristic optimization algorithms, the HS algorithm imposes fewer mathematical requirements and can be easily adopted for various types of engineering optimization problems [18, 19].

The optimization procedure of the HS algorithm consists of steps 1-5, as follows:

Step 1: Initialize the optimization problem and algorithm parameters.

Step 2: Initialize the harmony memory (HM).

Step 3: Improvise a new harmony from the HM.

Step 4: Update the HM.

Step 5: Repeat Steps 3 and 4 until the termination criterion is satisfied.

Due to its effectiveness in searching nonlinear, multi-dimensional search spaces, HS can be applied to the tuning of PI speed controller gains to ensure optimal control performance at nominal operating conditions.

IV. SIMULATION RESULTS

In order to analyse the driving wheel system behaviour, Simulations were carried using the model of Fig 2. The following results were simulated in MATLAB/SIMULINK.

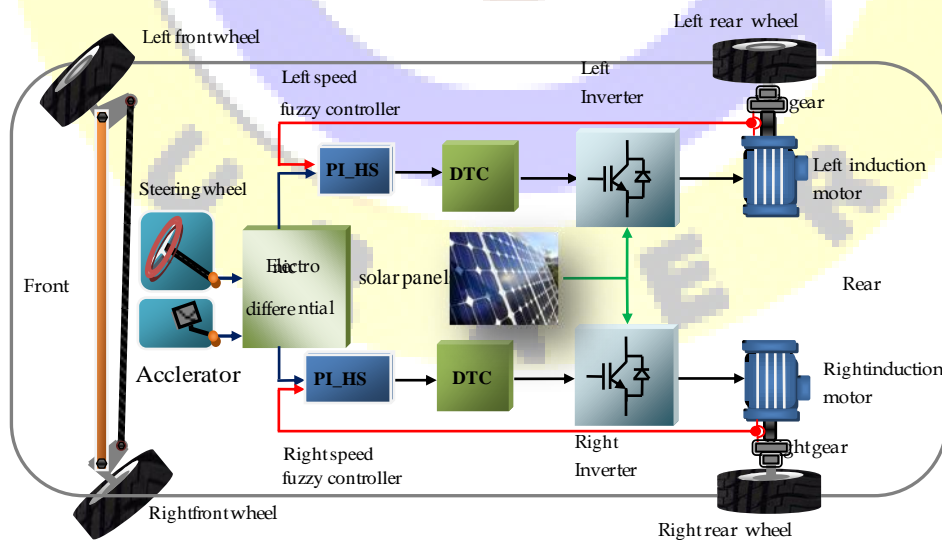


Fig. 2 The Driving Wheels Control System.

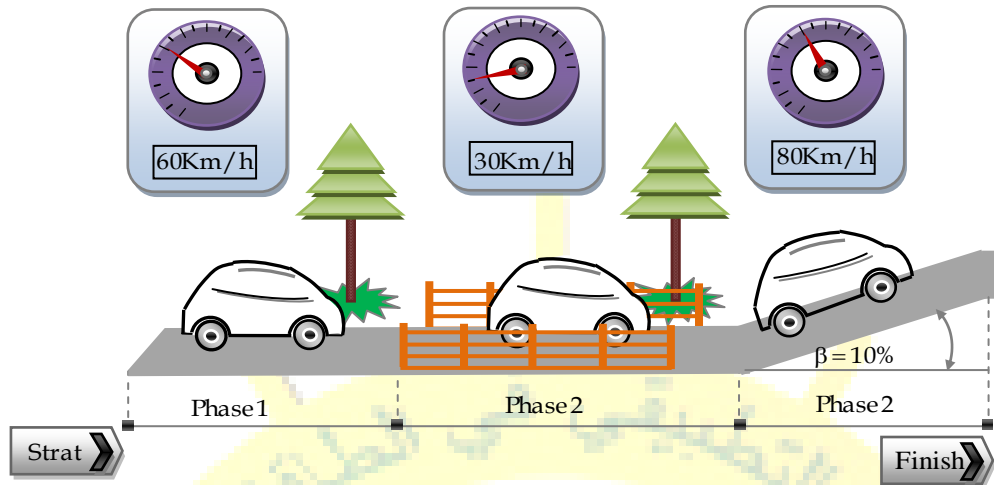


Fig.3.Specify driving route topology

a) Case of classical PI-controller

The initial values parameters of ant colony optimisation are shown in table below.

TABLE.II INITIAL VALUES PARAMETERS OF ACO

Ant Number	20
Maximum Cycle Time	100
Initial Value of Nodes Trail Intensity	0.1
Coefficient ρ	0.6
Relative Important Parameter of Trail Intensity α	3
Relative Important Parameter of Visibility β	2

The topology studied in this present work consists of three phases: the first one represent the acceleration phase's beginning with 60 Km/h in straight road, the second phase represent the deceleration one when the speed became 30 Km/h, and finally the EV is moving up the slopped road of 10% under 80 Km/h, the specified road topology is shown in Fig. 3, when the speed road constraints are described in the Table 3.

TABLE III. SPECIFIED DRIVING ROUTE TOPOLOGY

Phases	Event information	Vehicle Speed [km/h]
Phase 1	Acceleration	60
Phase 2	Bridge, Break	30
Phase 3	Acceleration and climbing a slope 10%	80

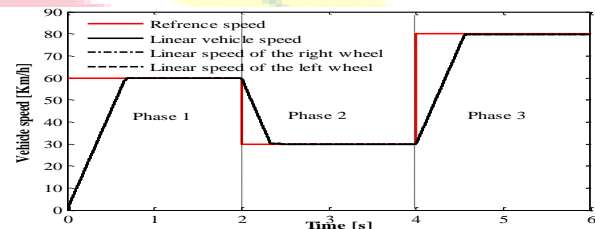


Fig. 4 Variation of vehicle speeds in different phases.

Refereed to Fig. 4 at time of 2 s the vehicle driver move on straight road with linear speed of 60 km/h, the assumption's that the two motors are not disturbed. In this case the driving wheels follow the same path with no overshoot and without error which can be justified with the good electronic differential act coupled with DTC performances.

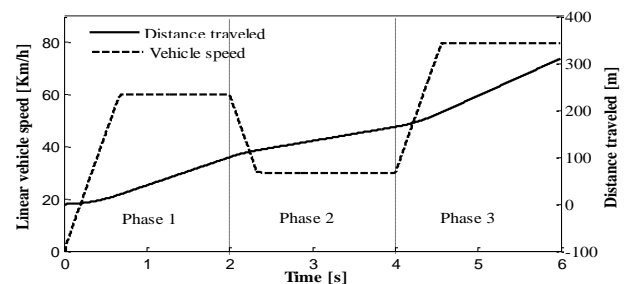


Fig. 5 Evaluation of vehicle and distance travelled in different phases.

Fig. 5, reflect the relationship between vehicle speed's variation and distance travelled in different phases. The distance travelled of 310 m in three electronic differential references acts 60 then break of 30 and acceleration until 80 km/h.

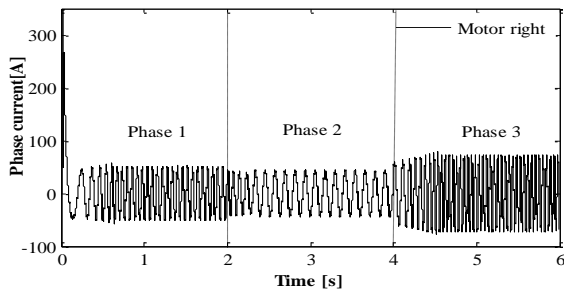


Fig. 6 Variation of phase current of the right motor in different phases.

Figs 6 and 7 explains the variation of phase current and driving force respectively. In the first step and to reach 60 km/h The EV demand a current of 50.70 A for each motor which explained with driving force of 329.30N. In second phase the current and driving forces demand decrees by means that the vehicle is in recharging phase's which explained with the decreasing of current demand and developed driving forces shown in Figs 6 and 7 respectively . The last phases explain the effect of acceleration under the slope on the straight road EV moving. The driving wheels forces increase and the current demand undergo double of the current braking phases the battery use the maximum of his power to satisfy the motorization demand under the sloped road condition which can interpreted physically the augmentation of the globally vehicle resistive torque illustrate in Table 4. In the other hand the linear speeds of the two induction motors stay the same and the road drop does not influence the torque control of each wheels. The results are listed in Table 4.

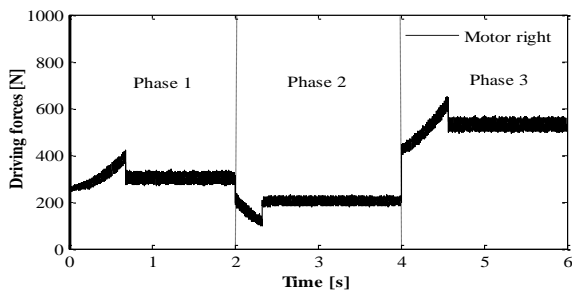


Fig. 7 Variation of driving force of the right motor in different phases.

TABLE IV. VARIATION OF VEHICLE TORQUE IN DIFFERENT PHASES.

Phases	1	2	3
the Vehicle resistive torque [N.m]	95.31	68.53	168.0
the globally vehicle resistive torque Percent compared with nominal motor torque of 476 Nm [%]	20.02	14.39	35.29

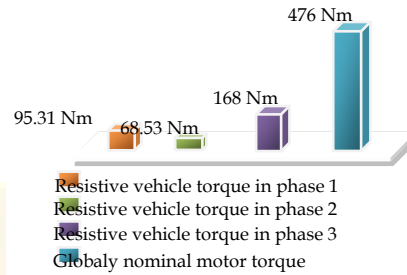


Fig.19. Evaluation of the globally vehicle resistive torque compared to nominal motor torque in different phases.

According to the formulas (2),(3),(4) and Table. 4, the variation of resistive vehicle torques in different cases as depicted in Table 4. , the vehicle resistive torque was 95.31 N.m in the first case (acceleration phase) when the power propulsion system resistive one is only 68.53 Nm in the breaking phases (phases 2) , the back driving wheels develop more and more efforts to satisfy the traction chain demand which impose an resistive torque equal to 168.00 N.m. The result prove that the traction chain under acceleration demand develop the double effort comparing with the breaking phase case's by means that the vehicle needs the half of its energy in the deceleration phase's compared with the acceleration one's as it specified in table 2.

b) Case of PI-ACO controller

The performance index in the Ant colony optimization is the Integral Time Absolute Error (ITAE) of speed error and rise time. As a consequence, F , the objective function, is defined by Equation 9:

$$\text{Minimize } F_v = \int (error)dt + tr \quad (9)$$

We can summaries the vehicle speed results in the following tables:




Le 3^{ème} Séminaire International sur les Energies Nouvelles et Renouvelables

The 3rd International Seminar on New and Renewable Energies

Unité de Recherche Appliquée en Energies Renouvelables,
Ghardaïa – Algérie 13 et 14 Octobre 2014



TABLE .IIV PERFORMANCES OF THE PI AND ANT PI OPTIMIZATION CONTROLLERS IN THE SPEED RESPONSE.

PI non optimized	PI optimized	
		
Parameter and indexes	PI non optimized	PI optimized
Overshoot [%]	0.5600	0.0133
Rise time (sec)	0.7087	0.6973
Steady state error [%]	1.0182e+001	6.7543e+000

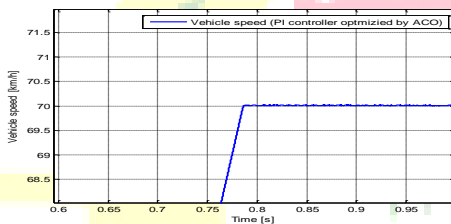


Fig. 8 The vehicle speed response of PI-AHS controller

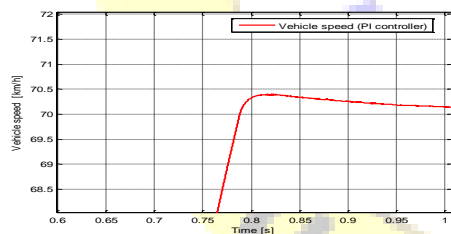


Fig. 9 The vehicle speed response of PI controller

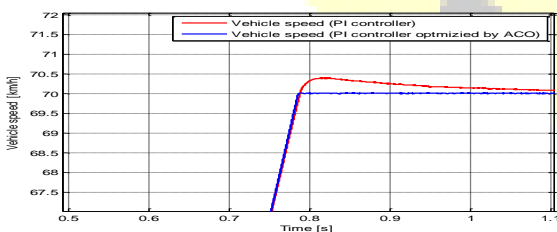


Fig. 10 The vehicle speed for PI and PI-HS controller.

To compare the effect of disturbances on the vehicle speed in the cases of two types of control, Figures 8,9,10 and table 5,

shows the system response in two cases (PI-HS and PI classical control), we can say that: the effect of the disturbance is neglected in the case of the PI_{HS}. It appears clearly that the classical control with PI controller is easy to apply. However, the control with the Ant colony optimization controllers offers better performances in both of the overshoot control and the tracking error.

In addition to these dynamic performances, it respects the imposed constraints by the driving system such as the robustness of parameter variations.

Table 5 prove that the ant PI-HS minimize the aerodynamic torque leading to the decrease of the front section of the electric vehicle.

The diminution of aerodynamic torque using ant PI-HS implique augmentation of autonomy battery power.

TABLE VIII COMPARATIVE STUDY

PI non optimized	PI optimized	
Parameter and indexes	PI non optimized	PI optimized
Aerodynamic torque [Nm]	51.0972	50.5370
Vehicle torque [Nm]	88.99	88.43
Current [A]	54.93	54.08
Electromagnetic torque [Nm]	126.50	125.63

V. CONCLUSION.

The research outlined in this paper has demonstrated the feasibility of an improved vehicle stability which utilises two independent back drive wheels for motion by using the direct torque control. This paper proposes an independent machine control structure applied to a propulsion system ensuring by the electronic differential. The results obtained by simulation show that this structure permits the realization of the robust control based on PI harmony search system, with good dynamic and static performances for the multi-converters/multi-machines propulsion system. The proposed PI-HS controller system improve the driving wheels speeds control with high accuracy either in flat roads or sloped ones. The disturbances do not affect the performances of the driving motors and the control law's efficiency gives a good dynamic characteristics of the traction chain.

VIII. Acknowledgment

This work is prepared to be presented in the The 3rd International Seminar on New and Renewable Energies which had in Ghardaïa – Algérie 13 et 14 Octobre 2014 So all my acknowledgment to our colleague of Renewable Energies, and the Editor in Chief and every body who helps us to prepare this paper and to success this conference.



**Le 3^{ème} Séminaire International sur les Energies Nouvelles et
Renouvelables**
**The 3rd International Seminar on New and Renewable
Energies**

**Unité de Recherche Appliquée en Energies Renouvelables,
Ghardaïa – Algérie 13 et 14 Octobre 2014**



REFERENCES

- [1] Y. P. Yang, C. P. Lo. Current Distribution Control of Dual Directly Driven Wheel Motors for Electric Vehicles. *Control Engineering Practice*, vol. 16, no. 11, pp. 1285-1292, 2008.
- [2] P. He, Y. Hori, M. Kamachi, K. Walters, H. Yoshida. Future Motion Control to be Realized by In-wheel Motored Electric Vehicle. In *Proceedings of the 31st Annual Conference of the IEEE Industrial Electronics Society*, IEEE Press, Raleigh South Carolina, USA, pp. 2632-2637, 2005.
- [3] Kang J. K., Sul S. K., New Direct Torque Control of Induction Motor for Minimum Torque Ripple and Constant Switching Frequency. *IEEE Trans. Ind. Applicat.*, vol. 35, no. 5, p. 1076-1082, 1999.
- [4] C. C. Chan et al., "Electric vehicles charge forward," *IEEE Power Energy Mag.*, vol. 2, no. 6, pp. 24-33, 2004.
- [5] Z. Zhu et al., "Electrical machines and drives for electric, hybrid, and fuel cell vehicles," *Proc. IEEE*, vol. 95, no. 4, pp. 764-765, 2007.
- [6] P. Vas, *Sensorless Vector and Direct Torque Control*, Oxford University Press, 1998.
- [7] K. Itoh and H. Kubota, "Thrust ripple reduction of linear induction motor with direct torque control," *Proceedings of the Eighth International Conference on Electrical Machines and Systems, ICEMS 2005*, vol. 1, pp. 655-658, 2005.
- [8] Chen, L., Fang, K.L.: A Novel Direct Torque Control for Dual-Three-Phase Induction Motor. *Conf. Rec. IEEE International Conference on Machine Learning and Cybernetics*, pp. 876-88, 2003.
- [9] A. Schell, H. Peng, D. Tran, E. Stamos, "Modeling and Control Strategy development for Fuel Cell Electric Vehicle", *Annual Review in control Elsevier*, Vol. 29, pp. 159-168, 2005.
- [10] A. Haddoun, Modeling, Analysis and neural network control of an EV Electrical Differential, *TRANSACTION ON industrial electronic* Vol. 55, N 6 June 2008.
- [11] A. Nasri, A. Hazzab, I.K. Bousserhane, S. Hadjeri, P. Sicard, Two Wheel Speed Robust Sliding Mode Control For Electric Vehicle Drive, *Serbian Journal of Electrical Engineering*, vol. 5, no.2, pp. 199-216, 2008.
- [12] K. HARTANI, Electronic Differential with Direct Torque Fuzzy Control for Vehicle Propulsion System, *Turk J Elec Eng & Comp Sci*, vol.17, no.1, 2009, TUBITAK.
- [13] L.T. Lam, R. Lovey, *Developpement of ultra-battery for hybrid-electric vehicle applications*, Elsevier, power sources, vol. 158, pp. 1140-1148, 2006.
- [14] Larminie, "Electric Vehicle Technology Explained", Edited by John Wiley and John Lowry, England, 2003.
- [15] A. Haddoun et al, Analysis modeling and neural network of an electric vehicle, in *Proc IEEE IEMDC, Antalya Turkey*, pp.854-859, 2007.
- [16] M. Vasudevan, R. Arumugam, "New direct torque control scheme of induction motor for electric vehicles," *5th Asian Control Conference*, vol. 2, pp. 1377 - 1383, 2004.
- [17] M. E. H. Benbouzid et al., "Advanced fault-tolerant control of induction motor drives for EV/HEV traction applications: From conventional to modern and intelligent control techniques," *IEEE Trans. Veh. Technol.*, vol. 56, no. 2, pp. 519-528, Mar. 2007.
- [18] Kim J.H., Geem Z.W., Kim E.S., "Parameter estimation of the nonlinear Muskingum model using harmony search", in *Journal American Water Resources Association*, vol. 37, no. 5, 2001, pp.1131-8.
- [19] Lee K.S., Geem Z.W., "A new structural optimization method based on the harmony search algorithm", in *Comput. Struct.*, 82(9-10.2004), pp. 781-98